◆ Human Brain Mapping 36:2756–2766 (2015) ◆

Pathological Uncoupling Between Amplitude and Connectivity of Brain Fluctuations in Epilepsy

Zhiqiang Zhang,[1,2]* Qiang Xu,[1] Wei Liao,[1,3] Zhengge Wang,[1] Qian Li,[4] Fang Yang,[4] Zongjun Zhang,[1] Yijun Liu,[5] and Guangming Lu[1,2]*

[1]*Department of Medical Imaging, Jinling Hospital, Nanjing University School of Medicine, Nanjing, China*
[2]*State Key Laboratory of Analytical Chemistry for Life Science, Nanjing University, Nanjing, China*
[3]*Center for Cognition and Brain Disorders, Affiliated Hospital of Hangzhou Normal University, Hangzhou, China*
[4]*Department of Neurology, Jinling Hospital, Nanjing University School of Medicine, Nanjing, China*
[5]*Department of Psychiatry and Neuroscience, University of Florida, Gainesville, Florida*

Abstract: Amplitude and functional connectivity are two fundamental parameters for describing the spontaneous brain fluctuations. These two parameters present close coupling in physiological state, and present different alteration patterns in epilepsy revealed by functional MRI (fMRI). We hypothesized that the alteration of coupling between these two imaging parameters may be underpinned by specific pathological factors of epilepsy, and can be employed to improve the capability for epileptic focus detection. Forty-seven patients (26 left- and 21 right-sided) with mesial temporal lobe epilepsy (mTLE) and 32 healthy controls underwent resting-state fMRI scans. All patients were detected to have interictal epileptic discharges on simultaneous electroencephalograph (EEG) recordings. Amplitude-connectivity coupling was calculated by correlating amplitude and functional connectivity density of low-frequency brain fluctuations. We observed reduced amplitude-connectivity coupling associated with epileptic discharges in the mesial temporal regions in both groups of patients, and increased coupling associated with epilepsy durations in the posterior regions of the default-mode network in the right-sided patients. Moreover, we proposed a new index of amplitude subtracting connectivity, which elevated imaging contrast for differentiating the patients from the controls. The findings indicated that epileptic discharges and chronic damaging effect of epilepsy might both contribute to alterations of amplitude-connectivity coupling in different pivotal regions in mTLE. Investigation on imaging cou-

Additional Supporting Information may be found in the online version of this article.

Contract grant sponsor: Natural Science Foundation of China; Contract grant numbers: 81271553; 81422022; 81201155; 81201078; 61131003 and 81171328; Contract grant sponsor: 863 project; Contract grant number: 2014BAI04B05 and 2015AA020505; Contract grant sponsor: the China Postdoctoral Science Foundation; Contract grant number: 2013M532229.

*Correspondence to: Zhiqiang Zhang; Department of Medical Imaging, Jinling Hospital, 305 Eastern Zhongshan Rd., Nanjing 210002, China. E-mail: zhangzq2001@126.com or Guangming Lu; Department of Medical Imaging, Jinling Hospital, 305 Eastern Zhongshan Rd., Nanjing 210002, China.
E-mail: cjr.luguangming@vip.163.com

Received for publication 13 November 2014; Revised 23 March 2015; Accepted 23 March 2015.

DOI: 10.1002/hbm.22805
Published online 16 April 2015 in Wiley Online Library (wileyonlinelibrary.com).

pling provides synergistic approach for describing brain functional changing features in epilepsy. *Hum Brain Mapp 36:2756–2766, 2015.*

Key words: low-frequency brain fluctuations; functional MRI; epilepsy; functional connectivity; amplitude

INTRODUCTION

Rapidly expanding arrays of resting-state functional MRI (fMRI) approaches facilitate comprehensive understanding of spontaneous brain activity from various aspects [Fox and Raichle, 2007; Zhang and Raichle, 2010]. Interestingly, recent imaging studies have found that the resting-state human brain presents largely similar topological patterns in different functional domains [Anderson et al., 2014; Baria et al., 2013; Liang et al., 2013; Tomasi et al., 2013]. The convergences of imaging findings suggest ubiquitous coupling across the properties of neural activity. Investigation of imaging coupling provides synergistic and complementary strategy to assess physiological and pathological processes of human brain.

Amplitude [Zang et al., 2007] and functional connectivity [Biswal et al., 1995] are two fundamental fMRI parameters describing local and network properties of resting-state brain fluctuations, respectively [Fox and Raichle, 2007]. These two parameters present close coupling in physiological state [Baria et al., 2013; Tomasi et al., 2014], but show divergent alterations in mesial temporal lobe epilepsy (mTLE). For amplitude of low frequency fluctuation (ALFF), increase was found in the epileptogenic regions and decrease was in the default-mode regions [Ji et al., 2013; Zhang et al., 2010a]. For functional connectivity, decrease was found in both the regions associating with epileptic focus [Bettus et al., 2010] and the default-mode network (DMN) [Pittau et al., 2012; Widjaja et al., 2013; Zhang et al., 2010b]. We hypothesized that uncoupling of these parameters in mTLE may be underlain by specific pathological factors. Moreover, both increased ALFF [Zhang et al., 2010a] and decreased connectivity [Bettus et al., 2010; Morgan et al., 2012] in the temporal lobe have been suggested to have clinical implication for detection of epileptic focus in mTLE. Thus we considered that combining application of these two parameters may elevate the imaging contrast, and improve capability of resting-state fMRI for epileptic focus detection.

To test these hypotheses, we combined measures of amplitude and functional connectivity density (FCD) of low-frequency BOLD fluctuations, and assessed the alteration of amplitude-connectivity coupling in mTLE, which might provide synergistic approach to unravel the features of functional changes in epilepsy. Moreover, we proposed a new index by subtracting values of connectivity from amplitude of low-frequency fluctuations, and applied it to resting-state fMRI data for more effectively differentiating the patients from controls.

METHODS

Forty-seven patients with mTLE were included in this study, consisting of 26 patients with left- (ages: 29.5 ± 10.3 years [Mean $\pm$ std]; genders: 12 females and 14 males; epilepsy durations: 10.5 ± 9.3 years) and 21 patients with right-sided mTLE (ages: 27.8 ± 8.1 years; genders: 11 females and 10 males; epilepsy durations: 12.6 ± 8.0 years). They were selected from 64 patients underwent simultaneous EEG and fMRI, and had interictal epileptiform discharges (IEDs) during fMRI scans. Diagnosis and lateralization of mTLE was performed through a comprehensive evaluation, including seizure history and semiology, neurological examination, diagnostic MRI, and EEG records in all patients. All patients presented hippocampal sclerosis on structural MRI. Patients were compared to 32 healthy controls (HCs) (ages: 30.3 ± 9.1 years; genders: 17 females and 15 males), recruited from the staff of Jinling Hospital. Controls did not suffer from neurological or psychiatric disorders at the time of the study. There were no age ($P = 0.51$, one way-ANOVA) and gender ($P = 0.86$, Kruskal–Wallis ANOVA) differences among patient and control groups. This study was approved by the Medical Ethics Committee in Jinling Hospital, Nanjing University School of medicine. All examinations were carried out under the guidance of the Declaration of Helsinki 1975. Written informed consent was obtained from all the participants.

Simultaneous EEG and fMRI Data Acquisitions

The patients underwent simultaneous EEG and fMRI data acquisitions on a 32 channels MRI-compatible EEG (Brain Product, Munich, Germany, 5 kHz sampling rate) and a 3T MRI scanner (SIEMENS Trio, Erlangen, Germany). The patients were instructed to keep rest and not fall in sleep. Foam pads were used to help secure the EEG leads, minimize motion, and improve patient comfort. For EEG recording, FCz was set as the reference and electrocardiography was recorded using an electrode placed on the back. For MRI data scanning, the functional data were acquired using a T2*-weighted single-shot echo planar imaging sequence (TR/TE = 2,000 ms/40 ms, FA = 90°, matrix = 64 × 64, field of view = 24 × 24 cm, thickness/gap= 4.0 mm/0.4 mm, 30 transverse slices aligned along the anterior–posterior commissure, two sessions with each

consisting of 500 volume measurements, after excluding the first five volumes). Moreover, conventional T1 and T2-weighted images using spin echo sequence were acquired for radiological diagnosis, and high-resolution three-dimension (3D) T1-weighted anatomical images in sagittal orientation using a magnetization prepared rapid gradient-echo sequence TR/TE = 2,300 ms/2.98 ms, flip angle = 9°, field of view = 256 × 256 mm^2, voxel size = 1 × 1 × 1 mm^3). For the HCs, high-resolution structural and fMRI data were acquired. Each HC had one functional data session consisting of 250 volume measurements. The other scan protocols were identical to those for the patients. Nobody was fall into sleep during MRI scan.

Data Preprocessing

The EEG data was offline-processed to remove gradient and ballistocardiogram artifacts using the Brain Vision Analyzer 2.0 software. IEDs were marked independently by an experienced electroencephalographer (Q.L) and a neurologist (F.Y), disagreements about the IEDs markers were resolved by discussion. For matching with the data length of the controls, an fMRI subsession of 250 volumes was extracted for each patient under the guidance of EEG output. This fMRI subsession covered the maximal IEDs number during the two sessions (left/right mTLE: $3.7 \pm 3.3/3.3 \pm 2.7$ events of IEDs). The fMRI data preprocessing was performed using a resting-state fMRI pipeline of DPARSF [Yan and Zang, 2010]. After slice-timing adjustment and realignment for head-motion correction, data were realigned with corresponding 3D anatomical images and warped into the anatomical MNI152 template using 12 parameters affine linear transformation at a resolution of 3 × 3 × 3 mm^3 for normalization, and spatially smoothed with an isotropic Gaussian kernel (8 mm full width at half maximum). Subsequently, data were linear trend removed and temporal band-pass filtered (0.01–0.08 Hz). Several nuisance variables, including six head-motion parameters, the global brain signal, the averaged signal from white matter and ventricles, were removed by multiple linear regression analysis. Considering the potential effect of morphological alteration on functional data, the gray matter (GM) volume of each subject extracted from voxel-based morphometric analysis, was also regressed voxel-wisely. Moreover, we applied a GM mask to all fMRI data to exclude artifactual affection from non-GM voxels. This mask was generated from GM tissue probability greater than 20%. The GM tissue probability template was released as part of tissue priors in SPM8 (http://www.fil.ion.ucl.ac.uk/spm/software/spm8).

Data Analysis

FCD mapping

Global FCD mapping was calculated to measure the voxel-wise functional connectivity strength [Tomasi and Volkow, 2010; Zuo et al., 2012]. The number of functional connections was determined through Pearson correlations between time-varying signals of a voxel and those in other voxels using an arbitrary threshold $r = 0.3$; this correlation threshold was estimated with statistical significance $P < 0.05$, *FWE* correction [Zuo et al., 2012].

ALFF mapping

To calculate ALFF measure at each voxel, the time series was transformed to the frequency domain by using fast Fourier transform. The power spectrum was then computed and square root-transformed at each voxel. The averaged square root of activity in the low-frequency band (0.01–0.08 Hz) was taken as the ALFF [Zang et al., 2007].

FCD and ALFF calculations were performed both using a resting-state fMRI data analysis toolkit of REST (http://www.restfmri.net).

ALFF-FCD contrast analysis

To test the proposal that the opposite alterations of ALFF and FCD in epilepsy may elevate imaging contrast to differentiate patients from HC, we computed the contrast of FCD to ALFF. In each subject, ALFF and FCD were firstly normalized by dividing the full-brain mean values of each parameter, in order to scale the values of these two parameters to an identical level. Subsequently, map of FCD was subtracted from that of ALFF, and then divided FCD plus ALFF for normalization (FCD−ALFF/FCD+ALFF) [Bianchin et al., 2011; Lee et al., 2000]. The calculation was performed voxel-by-voxel, and then produced an ALFF-FCD contrast map.

Relationship between ALFF and FCD

To describe the features of "uncoupling" between ALFF and FCD in mTLE, we investigated the relationship between these two parameters. In line with previous studies performing across-modality analysis [Anderson et al., 2014; Baria et al., 2013; Liang et al., 2013], we conducted correlation analyses across subjects and across voxels to quantitatively evaluate the relationship between ALFF and FCD. For each subject, both ALFF and FCD values were first standardized to z scores so that they could be averaged and compared across subjects [Liang et al., 2013]. Across-subject correlation analysis was performed at each voxel to investigate the relationship between ALFF and FCD in the patient group and HC group, respectively.

Across-voxel correlation analyses were performed at group level and individual level. At group level, ALFF and FCD values were averaged within each group, respectively, and then were correlated voxel-by-voxel within the whole brain and three specific regions, respectively. These specific regions were selected according to group comparison outputs (see the Results section), including the mesial temporal lobes, regions of the parietal cortices and posterior cingulate cortex, and the precentral cortices. For

individual level, correlation was calculated in each subject. For computational efficiency [Liang et al., 2013], we down-sampled the data to 6-mm isotropic voxels (a total of 5,025 voxels in GM).

Group comparisons

Group comparisons were performed to investigate the alteration of each imaging parameter in mTLE relative to HCs. The ALFF, FCD, and ALFF-FCD contrast maps of each patient group was compared with those of the control group using one way ANOVA implemented in SPM8. All the statistical maps were corrected for multiple comparisons to a significant level of $P < 0.05$ by combining the individual voxel $P < 0.01$ with cluster size >1,350 mm^3 based on using Monte Carlo simulations [Ledberg et al., 1998].

Moreover, we performed a confirmatory test using regions-of-interest (ROI)-based comparison of each imaging parameter within the mesial temporal structures (including the hippocampus and parahippocampal gyrus ipsilateral to the epileptogenic side, which was identified according to the AAL templates [Tzourio-Mazoyer et al., 2002]). The averaged scores within the ROIs of each imaging parameter underwent two-sample *t*-test analysis between the patient and control groups. The individual subject data were also plotted as a scattergram, which was used to select a cutoff point in the parameter scores that provided the optimal sensitivity and specificity in distinguishing patients from HCs [Greicius et al., 2004; Zhang et al., 2010a].

To test whether the spatial coupling (i.e., across-subject correlation between ALFF and FCD) were significantly different between the patient and control groups, correlation coefficients were converted into *z* values by using Fisher's *r*-to-*z* transform. This transformation generated values that were normally distributed. A *z* statistic was then used to compare these transformed *z* values to determine the significance of the between-group differences in correlations [He et al., 2008] FDR correction at *q* value of 0.05).

Moreover, one way ANOVA were employed to compare the across-voxel correlation coefficients (after Fisher's *r*-to-*z* transformation) between patients and controls using software of SPSS 17.0.

Correlations with pathological factors

Pathological factors of the IEDs numbers and epilepsy durations were correlated with ALFF and FCD in the patient groups using multiple regression analyses, which were assumed to reflect the effects of epileptic discharges and chronic damaging effects caused by epilepsy, respectively. These two factors were cross-regressed in the multiple regression models ($P < 0.05$, multiple correction using Monte Carlo simulations by combining the individual voxel $P < 0.01$ with cluster size >243 mm^3, constrained by mask produced from one-way ANOVA comparison). Moreover, to investigate the pathological effects on the ALFF-FCD coupling strengths (i.e., correlation coefficients between two imaging parameters), these two pathological factors were further correlated with the individual across-voxel correlation coefficients within the whole brain and specific regions using *Pearson* correlation. To account for the potential influence of outliers, we also used the *Shepherd pi* correlation analysis [Schwarzkopf et al., 2012].

RESULTS

Comparing Results of Imaging Parameters

Supporting Information sFigure 1 showed the group result of ALFF and FCD in each group conducted by one sample *t*-test. For two-sample *t*-test comparisons between patients and controls (Fig. 1, Table I): (1) *ALFF*. Increase was distributed in the bilateral mesial temporal lobes with predominance in the ipsilateral side to epileptogenic focus, the bilateral precentral gyri and the thalamus; decrease was located in the bilateral parietal cortices, post cingulate cortex and lateral temporal cortex. (2) *FCD*. Decrease was distributed in the bilateral mesial temporal lobes with predominance in the ipsilateral side to epileptogenic focus, posterior cingulate cortex, lateral temporal and parietal lobes; Increased FCD was located in the bilateral precentral gyri. Visual inspections revealed that reverse alterations of ALFF and FCD was located in the mesial temporal structures. Consistent increases of ALFF and FCD were located in the bilateral precentral gyri, and consistent decreases were mostly located in the default mode regions, including the posterior cingulate cortex, lateral temporal cortex and parietal cortex. Thus, the overlaps between increased ALFF and decreased FCD in the mesial temporal structures, consistent increases of ALFF and FCD in the precentral cortices, and consistent decreases of ALFF and FCD in the parietal cortex were selected as ROIs. These three ROIs were used as mask to constrain the post hoc across-voxel correlations between ALFF and FCD. (3) *ALFF-FCD contrast map*. Increased value was located in the bilateral mesial temporal structures (predominance in the ipsilateral side to epileptogenic focus), which is stronger than either the single ALFF or FCD outputs.

ROI based analyses revealed that there were significant differences in each imaging parameters between the patients and HCs. Moreover, scattergram showed that the parameters of ALFF-FCD (accuracy = 0.95 for LmTLE vs. HC, and accuracy = 0.92 for RmTLE vs. HC. Accuracy was defined by averaged scores of sensitivity and specificity) could more effectively differentiate the patients from the HCs than parameter of ALFF (accuracy = 0.82 for LmTLE vs. HC, and accuracy = 0.80 for RmTLE vs. HC) or FCD (accuracy = 0.78 for LmTLE vs. HC, and accuracy = 0.75 for RmTLE vs. HC) (Fig. 2, Table II).

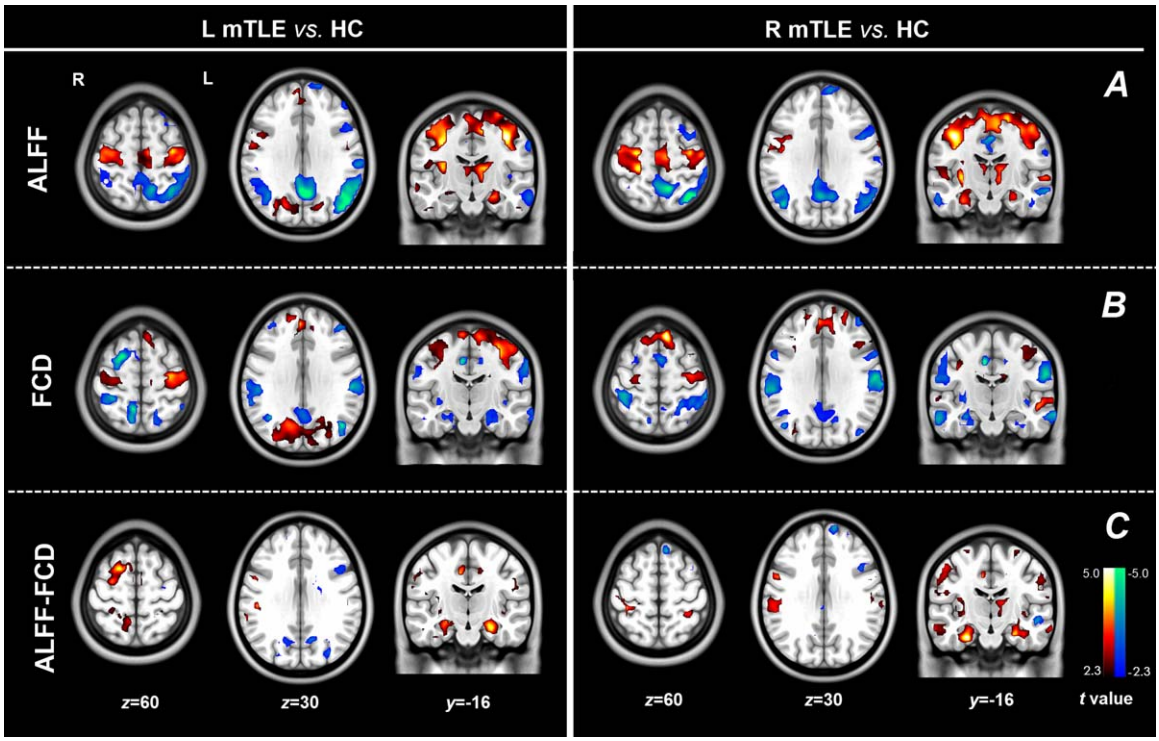

Figure 1.

Comparing results of imaging parameters between mTLE patients and HCs. Group comparison of ALFF (A) and FCD (B). In the patients with mTLE, opposite alterations of ALFF (increase) and FCD (decrease) were found in the mesial temporal lobes and insula; consistent decreases of ALFF and FCD was found in the regions of the default-mode network; and consistent increases was found in the precentral cortices. Moreover, increased ALFF was also found in the thalamus. (C) Group comparison of ALFF-FCD contrast map showed more pronounced group differences in the mesial temporal lobes. [Color figure can be viewed in the online issue, which is available at wileyonlinelibrary.com.]

Altered Coupling Between ALFF and FCD in the Patients

Across-subject correlation analyses between ALFF and FCD revealed widely distributed positive correlation in the midline and lateral cortical structures in the either healthy or patient groups. In the patient groups, the temporal structure ipsilateral to epileptogenic side showed weak coupling strength. Compared with the HCs, the patients showed decreased correlation between ALFF and FCD in the mesial temporal structures of epileptogenic side, and increased correlation in the posterior cingulate cortex (Fig. 3).

In the averaged group level, across-voxel correlation analyses showed positive correlations between ALFF and FCD in the whole brain and each ROI (Supporting Information sTable 1). In the individual level, the patients showed increased correlation strengths in the parietal cortex and decreased correlation strengths in the mesial temporal structures (Table III). Moreover, ALFF-FCD coupling strengths within the mesial temporal structures were negatively correlated with the numbers of IEDs in both patient groups (left-sided mTLE: *Pearson* correction: $r = -0.39$, $P < 0.05$;no correlation in Shepherd *pi* correlation analysis: $pi = -0.33$, $P = 0.24$. right-sided mTLE: *Pearson* correction: $r = -0.49$, $P < 0.05$ Shepherd pi correlation: $pi = -0.68$, $P < 0.01$); and ALFF-FCD coupling strengths within the default mode regions were positively correlated with epilepsy durations in the right mTLE patients (*Pearson* correction: $r = 0.52$, $P < 0.01$; Shepherd *pi* correlation: $pi = 0.46$, $P < 0.05$) (Fig. 4).

Correlations with Pathological Factors

Correlations with numbers of IEDs. The mesial temporal structures (mostly ipsilateral to the epileptogenic side) showed positive correlation with ALFF, and negative correlation with FCD. The posterior cingulate cortex and parietal cortex showed negative correlation with both ALFF and FCD.

Correlation with epilepsy durations. Negative correlation was found in the mesial temporal structures, posterior

TABLE I. Comparing results of fMRI parameters between patients and controls

	L mTLE versus HC (MNI: *x*, *y*, *z*; peak *t* values)			R mTLE versus HC (MNI: *x*, *y*, *z*; peak *t* values)		
Brain regions	ALFF	FCD	ALFF-FCD contrast	ALFF	FCD	ALFF-FCD contrast
LmTL	−33, −28,24; 5.85	−24, −30, −21; −3.66	−27, −30, −21; 6.68	−24, −27, −15; 2.96	−21, −12, −27; −2.74	−24, −27, −18; 4.18
RmTL	33, −27, −24; 4.18	21, −18, −24; −2.17	30, −21, −21; 5.58	27, −30, −9; 3.59	27, −15, −20; −3.16	30, −27, −24; 5.68
L lTL	−60, −39, −6; −4.89	−54,0, −27; −5.27	−51,9, −33; 4.71	−57, −12, −18; −3.77	−60, −3, −20; −3.82	−42,12, −39; 3.99
R lTL	60, −39, −6; −3.54	57,0, −27; −3.68	48, −3, −33; 2.65	60, −12, −24; −4.78	60, −9, −24; −5.64	54, −3, −39; 6.32
L ins	−36,3, −12; 4.41	−39, −3, −12; −4.08	−39, −3, −12; 4.65	−36,3, 12; 3.11	−39, 0, −12; −2.58	−39,0, −12; 3.54
R ins	33,6, −12; 4.00	42, −3, 9; −3.19	39, −6, −9; 3.23	33,3, −12; 4.91	45, −3,6; −4.54	39, −6, 9; 5.08
L Tha	16, −9,9; 5.08	—	—	−15, −12,18; 4.04	—	−12, −18,9; 2.98
R Tha	9, −9,9; 3.69	—	—	9, −18,9; 2.89	—	—
PCC	0, −60,33; −6.90	−1, −58, 33; −4.35	−6, −54,36; −3.05	3, −63, 30; −4.46	−9, −48,51; −3.23	3, −72,39; −3.47
L IPS	−42, −66,30; −5.79	−42, −69,27; −4.17	—	−27, −51,48; −3.28	−39, −60,39; −3.62	—
R IPS	42, −69,30; −4.24	39, −60,27; −3.80	—	27, −45, 45; −3.70	48, −75, 27; −4.06	—
L IPL	−57, −51,39; −6.62	−36, −39,48; −3.53	—	−39, −60,33; −3.30	−36, −45,51; −3.25	—
R IPL	−51, −42,48; −3.64	−33, −39,45; −4.23	—	45, −72, 27; −4.51	39, −36,54; −3.33	—
L PCA	−36, −18,48; 5.50	−33, −15,54; 4.11	—	−36, −21,48; 3.74	−33, −21,45; 2.39	—
R PCA	36, −18,42; 4.92	33, −21, 54; 2.46	—	45, −12,51; 5.86	39, −15,33; 3.60	—

LmTL: left mesial temporal lobe, RmTL: right mesial temporal lobe, L lTL: left lateral mesial temporal lobe, R lTL: right lateral temporal lobe, L ins: left insula, R ins: right insula, PCC: posterior cingulate cortex, L IPS: left intra-parital sulus, R IPS: right intra-parital sulus, L IPL: left inferior parietal lobular, R IPL: right inferior parietal lobular, L PCA: left precentral area, R PCA: right precentral area; L mTLE: left-sided mesial temporal lobe epilepsy, R mTLE: right-sided mesial temporal lobe epilepsy, HC: Healthy controls; ALFF: amplitude of low-frequency fluctuation, FCD: functional connectivity density.

cingulate cortex and parietal cortex for both ALFF and FCD. Positive correlation was found to be with the ALFF-FCD coupling strengths in the parietal cortex (Supporting Information sFigure 2).

DISCUSSION

By combining fMRI parameters of ALFF and FCD, we comprehensively assessed alteration patterns of resting-state brain activity in mTLE. We found that the amplitude-connectivity was reduced and were mildly correlated with epileptic discharges in the mesial temporal regions in both groups of patients, and increased coupling was correlated with epilepsy durations in the posterior regions of the DMN in the right-sided mTLE. Moreover, based on divergence of ALFF and FCD alterations in mTLE, we proposed a new imaging index of ALFF-FCD contrast by subtracting connectivity from amplitude, which elevated imaging contrast for differentiating the patients from the controls than using single index of ALFF or FCD.

ALFF and FCD are two prevalent fMRI indices for describing the characteristics of resting-state brain activity from different aspects. ALFF depicts the local property of brain activity by measuring averaged deviation of fMRI fluctuations during a short period of time [Zang et al., 2007], and reflects brain energetic metabolism [Tomasi et al., 2013]. FCD unbiasedly measures functional connectivity strength over the whole brain using graph-theory way, and reflects the communication amounts [Tomasi and Volkow 2010; Tomasi et al., 2013, 2014]. In the present study, we for the first time demonstrated specific alteration patterns ALFF and FCD in epilepsy, which offer a more complete picture of brain function disrupted by disease.

We found opposite alterations between ALFF and FCD in the epileptogenic regions in the patients. In line with our previous studies [Ji et al., 2013; Zhang et al., 2010a], the mesial temporal structures showed increased ALFF, and the ALFF value was positively correlated with epileptic discharges in these regions. Interictal epileptic discharges can induce specifically positive and negative BOLD responses [Benar et al., 2002; Kobayashi et al., 2006a], then the signal deviations would increase the amplitude values of BOLD fluctuations, which has been identified in our previous study [Zhang et al., 2010a]. In addition, given the evidence that ALFF is linear correlated with energetic metabolism [Tomasi et al., 2013], we proposed that increased ALFF in the mesial temporal structures might reflect the "core of interictal hypermetabolism" of epileptogenic region [Nelissen et al., 2006; Witte et al., 1994]. Moreover, decreased FCD was found in the mesial temporal structures, which was negatively correlated with epileptic discharges and epilepsy duration. Decreased functional connectivity in epilepsy has been interpreted as functional impairment due to damaging

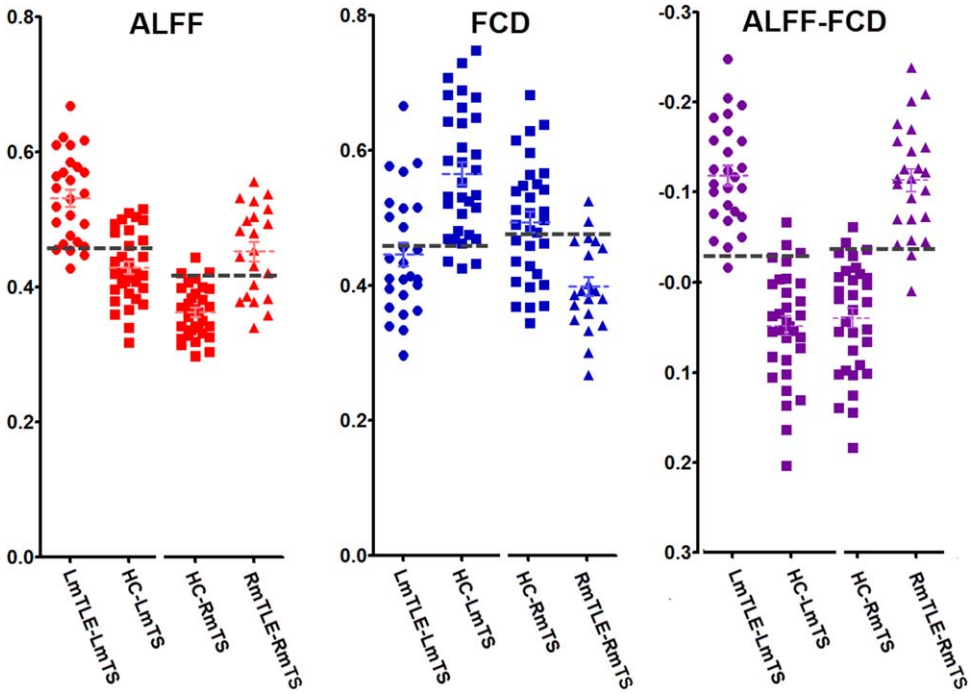

Figure 2.

Individual scores for imaging parameters in the mesial temporal structures ipsilateral to epileptogenic. There were significant group differences of each imaging parameter between patients and HCs. Scattergrams show that parameter of ALFF-FCD contrast could yield higher accuracy for differentiating the patients from HC than a single parameter of ALFF or FCD. The dash line indicate a cutoff point. [Color figure can be viewed in the online issue, which is available at wileyonlinelibrary.com.]

effect from epilepsy [Bettus et al., 2010; Pittau et al., 2012; Zhang et al., 2010b]. In this study, we also proposed that decreased FCD might attribute to dyssynchronization between mesial temporal region and the whole brain, since the different BOLD responses to epileptic activity [Kang et al., 2003; Stefanovic et al., 2005] may lead to loss of BOLD signals synchronization in different brain regions. Moreover, chronic damaging effect of epilepsy might also contribute to decrease in FCD.

Significantly, the opposite alteration patterns of these two fMRI parameters provide a window for elevating imaging contrast to detect abnormalities in the epileptic

TABLE II. ROI-based analyses of imaging parameters for differentiating patients and healthy controls

		ALFF	FCD	ALFF-FCD
LmTLE versus HC	Comparison	t = 6.72; $P < 0.001$	$t = -4.93$; $P < 0.001$	$t = 10.61$; $P < 0.001$
	Differentiating	Se = 0.69, Sp = 0.96; Ac = 0.82 (CO = 0.447)	Se = 0.65, Sp = 0.46; Ac = 0.78 (CO = 0.463)	Se = 0.94, Sp = 0.96; Ac = 0.95 (CO = 0.029)
RmTLE versus HC	Comparison	$t = 6.27$; $P < 0.001$	$t = -4.29$; $P < 0.001$	$t = 8.67$; $P < 0.001$
	Differentiating	Se = 0.67, Sp = 0.94; Ac = 0.80 (CO = 0.421)	Se = 0.59, Sp = 0.90; Ac = 0.75 (CO = 0.477)	Se = 0.94, Sp = 0.90; Ac = 0.92 (CO = 0.032)

R mTLE: right-sided mesial temporal lobe epilepsy, HC: Healthy controls; ALFF: amplitude of low-frequency fluctuation, FCD: functional connectivity density. Se: sensitivity, Sp: specificity, Ac: Accuracy, defined by averaged scores of sensitivity and specificity, CO= cutoff point. Comparing analyses were performed using two-sample *t*-test, and differential analyses were performed by selecting a cutoff point, which providing the optimal sensitivity and specificity in distinguishing patients from HCs.

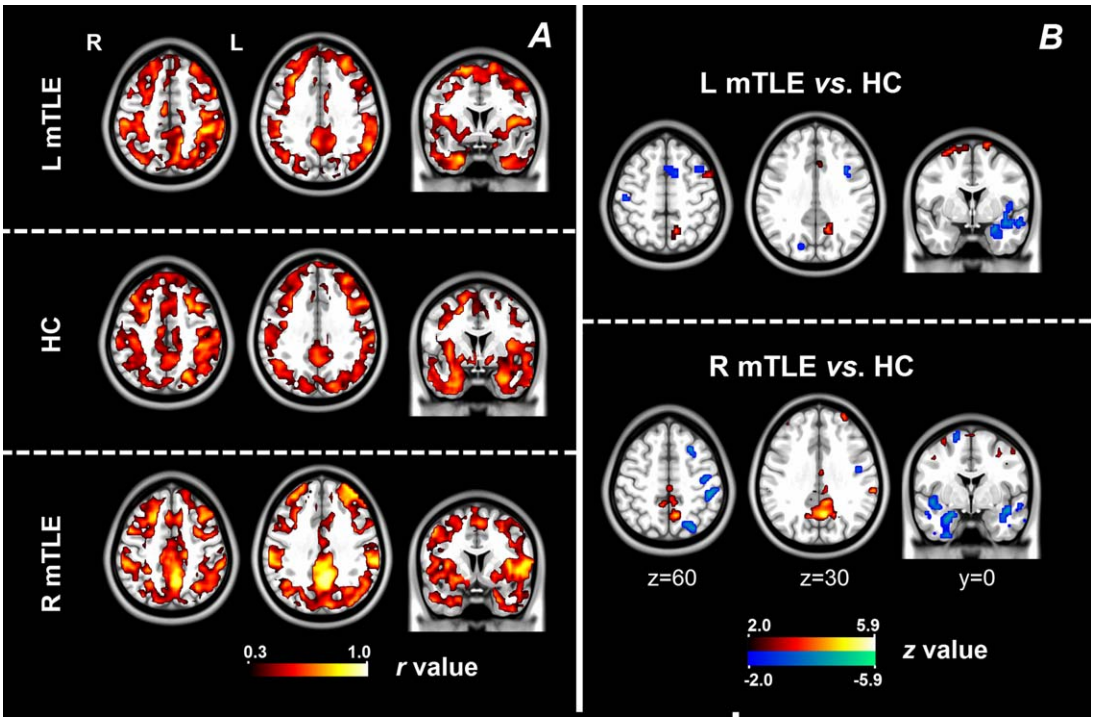

Figure 3.

Across-subject correlation between ALFF and FCD. (A) Coupling between ALFF and FCD was calculated using across-subject correlation in each subject group. Visual inspection revealed weaker coupling in the temporal lobe ipsilateral to epileptogenic side in the patient groups. (B) Comparing results of coupling between ALFF and FCD between patient groups and healthy group. The patients showed decreased coupling in the temporal lobe ipsilateral to epileptogenic side, and increased coupling in the posterior cingulate cortex. [Color figure can be viewed in the online issue, which is available at wileyonlinelibrary.com.]

regions. This phenomenon is in analogy with the strategy of subtracted ictal-interictal SPECT co-registered with MRI (SISCOM), which employs the uncoupling of ictal hyperperfusion and interictal hypoperfusion to more effectively localize epileptogenic focus [Bianchin et al., 2011; Lee et al., 2000]. Here, we proposed that subtracted amplitude-connectivity of BOLD fluctuations provides an noninvasive, fMRI-based imaging approach, and is more sensitive than either of the two single measures for epileptic region detection.

In contrast, wide distributed cortical structures showed consistent decreases in ALFF and FCD, including the lateral temporal lobe, parietal structures belonging to the posterior regions of the DMN [Fox et al., 2006; Raichle et al., 2001]. The DMN abnormalities in mTLE have been well-addressed in a large body of imaging studies [Laufs et al., 2007; Widjaja et al., 2013; Zhang et al., 2010b], which have been regarded as functional impairments caused by effects of interictal epileptic discharges suspension and [Gotman et al., 2005] chronic seizures damages [Zhang et al., 2010b]. In agreement with these previous studies, we found that the amplitude values in the DMN were both negatively correlated with epileptic discharges and epilepsy duration. The current findings might support the proposal that wide cortical structures are

TABLE III. Across-voxel correlation in individual level

Brain regions	HC (r)	LmTLE (r)	RmTLE (r)	ANOVA	LSD (LmTLE vs. HC); (RmTLE vs. HC)
Whole brain	0.32 ± 0.11	0.31 ± 0.14	0.30 ± 0.17	$F = 0.22$, $P = 0.80$	$P = 0.76$; $P = 0.51$
Mesial temporal lobe	0.30 ± 0.14	0.20 ± 0.17	0.24 ± 0.14	$F = 6.06$, $P < 0.05$*	$P < 0.01$*; $P < 0.05$*
Default-mode regions	0.23 ± 0.10	0.32 ± 0.15	0.31 ± 0.15	$F = 5.06$, $P < 0.05$*	$P < 0.05$*; $P < 0.05$*
Precentral cortices	0.27 ± 0.16	0.28 ± 0.18	0.30 ± 0.20	$F = 0.23$, $P = 0.79$	$P = 0.84$; $P = 0.50$

L mTLE: left-sided mesial temporal lobe epilepsy, R mTLE: right-sided mesial temporal lobe epilepsy, HC: Healthy controls.

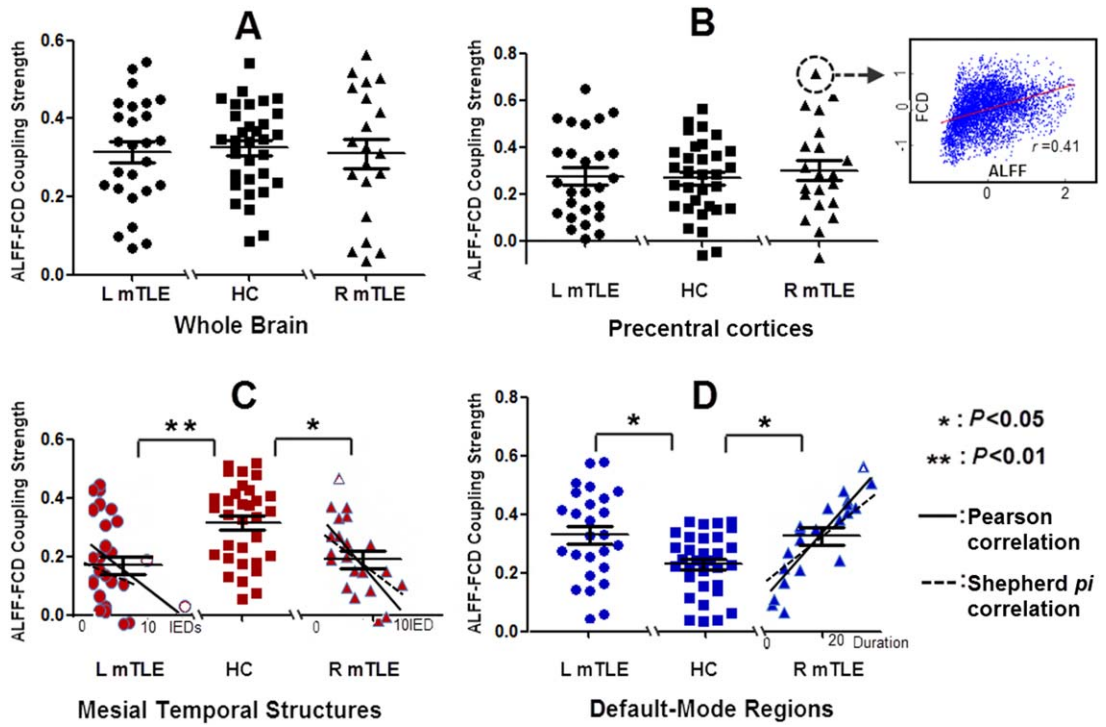

Figure 4.

Across-voxel correlation between ALFF and FCD. Coupling between ALFF and FCD was calculated using across-voxel correlation in individual. Coupling calculated within the whole brain (A) and the precentral cortex (B). There was no group difference of coupling strengths within the whole brain and precentral cortex. Group differences of coupling strengths within the mesial temporal structures. (C) and default-mode regions. (D) Moreover, ALFF-FCD coupling strengths within the mesial temporal structures were negatively correlated with numbers of IEDs in both patient groups (left-sided mTLE: *Pearson* correction: $r = -0.39$, $P < 0.05$;no correlation in Shepherd *pi* correlation analysis: $pi = -0.33$, $P = 0.24$. right-sided mTLE: *Pearson* correction: $r = -0.49$, $P < 0.05$ Shepherd *pi* correlation: $pi = -0.68$, $P < 0.01$); and ALFF-FCD coupling strengths within the default mode regions were positively correlated with epilepsy durations in the right mTLE patients (*Pearson* correction: $r = 0.52$, $P < 0.01$; Shepherd *pi* correlation: $pi = 0.46$, $P < 0.05$). [Color figure can be viewed in the online issue, which is available at wileyonlinelibrary.com.]

functionally impaired in mTLE [Kobayashi et al., 2006b; Laufs, 2012].

In addition, a few of other regions, which are frequently addressed in mTLE studies, showed various alteration patterns in these two imaging parameters. The insula showed increased ALFF and decreased FCD; while the thalamus showed significant increase in ALFF, but no difference in FCD. These structures are essential nodes involved in mesial temporal epilepsy network [Spencer, 2002], and associated with generation and propagation of epileptic activity [Blumenfeld, 2002; Isnard et al., 2000]. Moreover, the precentral cortices, as the primary motor areas, showed both increases in ALFF and FCD. These cortical regions were affected by seizures activity generated from hippocampus [van Rooyen et al., 2006], and might be associated with neocortical hyperexcitability in TLE [Silva et al., 2002]. However, it is currently not well understood about the pathophysiological mechanism underlying the different imaging alteration patterns across these regions.

Importantly, we further assessed alterations of amplitude-connectivity coupling by investigating the relationship between ALFF and FCD. These two parameters present close coupling with similar distribution patterns in physiological states [Baria et al., 2013; Tomasi et al., 2014], and the coupling could be modulated by different task loadings [Tomasi et al., 2014]. These studies suggested that the local fluctuations of BOLD in the brain are modulated by network-specific properties of connectivity [Baria et al., 2013]. In the present study, we found that the coupling between ALFF and FCD was decreased in the mesial temporal structures and increased in the posterior cingulate cortex in mTLE, and the coupling strengths in these regions were correlated with clinical factors. This finding indicated that the amplitude-connectivity coupling could be disrupted by pathological factors of epilepsy. Moreover, Tomasi and colleagues have recently correlated ALFF and FCD of fMRI signals with glucose metabolism, and further indicated that the regions showing higher energy demands

of brain communication might be more vulnerable to deficits in energy delivery or utilization [Tomasi et al., 2013]. Our results provided supplementary implication that the brain regions with abnormally high energy could also render to disruption of communication. The specific patterns of amplitude-connectivity uncoupling provided a novel depictor for presenting the pathological characteristic of functional changes in epilepsy.

Methodological Consideration and Limitations

With multiple analysis approaches, resting-state fMRI has been increasingly proven promising tool for depicting the features of epileptic activity. This study for the first time simultaneously applied two different parameters to fMRI data of mTLE patients. This strategy provided synergistic way for comprehensively assessing the features of functional changing in epilepsy. Moreover, the specific alteration patterns between these two parameters provided a more effective way to differential epileptic patients from normal controls. Whereas, several methodological considerations and limitations are noteworthy. First, various optional procedures during FCD calculation can lead to results diversification, which may render to different results [Stufflebeam et al., 2011]. Moreover, we only measured the global FCD, and did not specifically consider the local effects [Tomasi and Volkow, 2010]. Second, this work only involved the patients whom the lateralization diagnosis was already identified by other methods. It is required to test the practical value of this approach in epilepsy lateralization by applying it to patients with negative structural MRI in the future work. Third, our design does not allow us to control for confounding effects of antiepileptic drugs, which can affect normal neuronal function [Drane and Meador, 2002]. Fourth, the parameters ALFF and FCD are based on blood oxygenation level-dependent fluctuations, future study combining imaging modalities quantitative measuring physiological indices is needed. Fifth, the sample size of involved patients was rather small, future study with large patient sample is needed for validating the method reliability of this work.

CONCLUSION

In this study, we observed the specific alteration patterns of amplitude-connectivity coupling of low frequent fMRI fluctuations in mTLE. The findings indicate pathological factors lead to specific alterations of amplitude-connectivity coupling in the pivotal regions in mTLE. Moreover, we proposed a new index of amplitude subtracting connectivity, which elevated imaging contrast for epileptic focus detection. Investigation on imaging coupling provides synergistic approach to unravel the features of functional changes in epilepsy.

ACKNOWLEDGEMENTS

We thank Dr. Xi-nian Zuo, in the institute of psychology, CAS for his helpful suggestions. Author Contributions: Dr. Zhang recruited the subjects, collected the data, performed the analysis, generated the images, and wrote the manuscript. Dr. Liao and Q. Xu assisted with the analysis of data and generation of the figures. Dr. Wang and Dr. Yang assisted with data collections. Mrs. Li and Dr. Yang worked as electroencephalographer for EEG diagnosis. Dr. Zhang, Dr. Liu and Dr. Lu contributed to the development of the research concept. Disclosure: The authors report no disclosures. Potential conflicts of interest: Nothing to report.

REFERENCES

Anderson JS, Zielinski BA, Nielsen JA, Ferguson MA (2014): Complexity of low-frequency blood oxygen level-dependent fluctuations covaries with local connectivity. Hum Brain Mapp 35: 1273–1283.

Baria AT, Mansour A, Huang L, Baliki MN, Cecchi GA, Mesulam MM, Apkarian AV (2013): Linking human brain local activity fluctuations to structural and functional network architectures. Neuroimage 73:144–155.

Benar CG, Gross DW, Wang Y, Petre V, Pike B, Dubeau F, Gotman J (2002): The BOLD response to interictal epileptiform discharges. Neuroimage 17:1182–1192.

Bettus G, Bartolomei F, Confort-Gouny S, Guedj E, Chauvel P, Cozzone PJ, Ranjeva JP, Guye M (2010): Role of resting state functional connectivity MRI in presurgical investigation of mesial temporal lobe epilepsy. J Neurol Neurosurg Psychiatry 81:1147–1154.

Bianchin MM, Wichert-Ana L, Velasco TR, Martins AP, Sakamoto AC (2011): Imaging epilepsy with SISCOM. Nat Rev Neurol 7: 1–2.

Biswal B, Yetkin FZ, Haughton VM, Hyde JS (1995): Functional connectivity in the motor cortex of resting human brain using echo-planar MRI. Magn Reson Med 34:537–541.

Blumenfeld H (2002): The thalamus and seizures. Arch Neurol 59: 135–137.

Drane DL, Meador KJ (2002): Cognitive and behavioral effects of antiepileptic drugs. Epilepsy Behav 3:49–53.

Fox MD, Raichle ME (2007): Spontaneous fluctuations in brain activity observed with functional magnetic resonance imaging. Nat Rev Neurosci 8:700–711.

Fox MD, Corbetta M, Snyder AZ, Vincent JL, Raichle ME (2006): Spontaneous neuronal activity distinguishes human dorsal and ventral attention systems. Proc Natl Acad Sci U S A 103:10046–10051.

Gotman J, Grova C, Bagshaw A, Kobayashi E, Aghakhani Y, Dubeau F (2005): Generalized epileptic discharges show thalamocortical activation and suspension of the default state of the brain. Proc Natl Acad Sci U S A 102:15236–15240.

Greicius MD, Srivastava G, Reiss AL, Menon V (2004): Default-mode network activity distinguishes Alzheimer's disease from healthy aging: evidence from functional MRI. Proc Natl Acad Sci U S A 101:4637–4642.

He Y, Chen Z, Evans A (2008): Structural insights into aberrant topological patterns of large-scale cortical networks in Alzheimer's disease. J Neurosci 28:4756–4766.

Isnard J, Guenot M, Ostrowsky K, Sindou M, Mauguiere F (2000): The role of the insular cortex in temporal lobe epilepsy. Ann Neurol 48:614–623.

Ji GJ, Zhang Z, Zhang H, Wang J, Liu DQ, Zang YF, Liao W, Lu G (2013): Disrupted causal connectivity in mesial temporal lobe epilepsy. PLoS One 8:e63183.

Kang JK, Benar C, Al-Asmi A, Khani YA, Pike GB, Dubeau F, Gotman J (2003): Using patient-specific hemodynamic response functions in combined EEG-fMRI studies in epilepsy. Neuroimage 20:1162–1170.

Kobayashi E, Bagshaw AP, Grova C, Dubeau F, Gotman J (2006a): Negative BOLD responses to epileptic spikes. Hum Brain Mapp 27:488–497.

Kobayashi E, Hawco CS, Grova C, Dubeau F, Gotman J (2006b): Widespread and intense BOLD changes during brief focal electrographic seizures. Neurology 66:1049–1055.

Laufs H (2012): Functional imaging of seizures and epilepsy: Evolution from zones to networks. Curr Opin Neurol 25:194–200.

Laufs H, Hamandi K, Salek-Haddadi A, Kleinschmidt AK, Duncan JS, Lemieux L (2007): Temporal lobe interictal epileptic discharges affect cerebral activity in "default mode" brain regions. Hum Brain Mapp 28:1023–1032.

Ledberg A, Akerman S, Roland PE (1998): Estimation of the probabilities of 3D clusters in functional brain images. Neuroimage 8:113–128.

Lee HW, Hong SB, Tae WS (2000): Opposite ictal perfusion patterns of subtracted SPECT. Hyperperfusion and hypoperfusion. Brain 123(Pt 10):2150–2159.

Liang X, Zou Q, He Y, Yang Y (2013): Coupling of functional connectivity and regional cerebral blood flow reveals a physiological basis for network hubs of the human brain. Proc Natl Acad Sci U S A 110:1929–1934.

Morgan VL, Sonmezturk HH, Gore JC, Abou-Khalil B (2012): Lateralization of temporal lobe epilepsy using resting functional magnetic resonance imaging connectivity of hippocampal networks. Epilepsia 53:1628–1635.

Nelissen N, Van Paesschen W, Baete K, Van Laere K, Palmini A, Van Billoen H, Dupont P (2006): Correlations of interictal FDG-PET metabolism and ictal SPECT perfusion changes in human temporal lobe epilepsy with hippocampal sclerosis. Neuroimage 32:684–695.

Pittau F, Grova C, Moeller F, Dubeau F, Gotman J (2012): Patterns of altered functional connectivity in mesial temporal lobe epilepsy. Epilepsia 53:1013–1023.

Raichle ME, MacLeod AM, Snyder AZ, Powers WJ, Gusnard DA, Shulman GL (2001): A default mode of brain function. Proc Natl Acad Sci U S A 98:676–682.

Schwarzkopf DS, De Haas B, Rees G (2012): Better ways to improve standards in brain-behavior correlation analysis. Front Hum Neurosci 6:200.

Silva AV, Sanabria ER, Cavalheiro EA, Spreafico R (2002): Alterations of the neocortical GABAergic system in the pilocarpine model of temporal lobe epilepsy: Neuronal damage and immunocytochemical changes in chronic epileptic rats. Brain Res Bull 58:417–421.

Spencer SS (2002): Neural networks in human epilepsy: Evidence of and implications for treatment. Epilepsia 43:219–227.

Stefanovic B, Warnking JM, Kobayashi E, Bagshaw AP, Hawco C, Dubeau F, Gotman J, Pike GB (2005): Hemodynamic and metabolic responses to activation, deactivation and epileptic discharges. Neuroimage 28:205–215.

Stufflebeam SM, Liu H, Sepulcre J, Tanaka N, Buckner RL, Madsen JR (2011): Localization of focal epileptic discharges using functional connectivity magnetic resonance imaging. J Neurosurg 114:1693–1697.

Tomasi D, Volkow ND (2010): Functional connectivity density mapping. Proc Natl Acad Sci U S A 107:9885–9890.

Tomasi D, Wang GJ, Volkow ND (2013): Energetic cost of brain functional connectivity. Proc Natl Acad Sci U S A 110:13642–13647.

Tomasi D, Wang R, Wang GJ, Volkow ND (2014): Functional connectivity and brain activation: A synergistic approach. Cereb Cortex 24:2619–2629.

Tzourio-Mazoyer N, Landeau B, Papathanassiou D, Crivello F, Etard O, Delcroix N, Mazoyer B, Joliot M (2002): Automated anatomical labeling of activations in SPM using a macroscopic anatomical parcellation of the MNI MRI single-subject brain. Neuroimage 15:273–289.

van Rooyen F, Young NA, Larson SE, Teskey GC (2006): Hippocampal kindling leads to motor map expansion. Epilepsia 47: 1383–1391.

Widjaja E, Zamyadi M, Raybaud C, Snead OC, Smith ML (2013): Impaired default mode network on resting-state fMRI in children with medically refractory epilepsy. AJNR Am J Neuroradiol 34:552–557.

Witte OW, Bruehl C, Schlaug G, Tuxhorn I, Lahl R, Villagran R, Seitz RJ (1994): Dynamic changes of focal hypometabolism in relation to epileptic activity. J Neurol Sci 124:188–197.

Yan C, Zang Y (2010): DPARSF: A MATLAB toolbox for "pipeline" data analysis of resting-state fMRI. Front Syst Neurosci 4:13.

Zang YF, He Y, Zhu CZ, Cao QJ, Sui MQ, Liang M, Tian LX, Jiang TZ, Wang YF (2007): Altered baseline brain activity in children with ADHD revealed by resting-state functional MRI. Brain Dev 29:83–91.

Zhang D, Raichle ME (2010): Disease and the brain's dark energy. Nat Rev Neurol 6:15–28.

Zhang Z, Lu G, Zhong Y, Tan Q, Chen H, Liao W, Tian L, Li Z, Shi J, Liu Y (2010a): fMRI study of mesial temporal lobe epilepsy using amplitude of low-frequency fluctuation analysis. Hum Brain Mapp 31:1851–1861.

Zhang Z, Lu G, Zhong Y, Tan Q, Liao W, Wang Z, Li K, Chen H, Liu Y (2010b): Altered spontaneous neuronal activity of the default-mode network in mesial temporal lobe epilepsy. Brain Res 1323:152–160.

Zuo XN, Ehmke R, Mennes M, Imperati D, Castellanos FX, Sporns O, Milham MP (2012): Network centrality in the human functional connectome. Cereb Cortex 22:1862–1875.